

Electronic Ballast Based on the ZCS Class-E Amplifier

Balastro Electrónico Basado en un Amplificador Clase-E Conmutado a Corriente Cero

Mario Ponce¹, Rubén Vázquez¹, Jaime Arau¹ and J. Marcos Alonso²

¹Centro Nacional de Investigación y Desarrollo Tecnológico (CENIDET)

P. Box 5-164, CP. 62050, Cuernavaca, México

²Universidad de Oviedo, Área de Tecnología Electrónica

Campus Viesques s/n 33204, Gijón, España

E-mails: ponce@cenidet.edu.mx, marcos@ate.uniovi.es

Article received on June 15, 2001; accepted on Febrero 19, 2002

Abstract

In this paper a Zero-Current-Switching (ZCS) class-E amplifier is proposed as fluorescent lamp ballast. The ZCS class E amplifier features lower voltage stress across the switch than the Zero-Voltage-Switching (ZVS) class E amplifier. This is an important advantage, which allows to supply the circuit from the American main voltage ($V_{ac}=120\text{ V}$), maintaining only one switch for the ballast. The operation and characteristics of the ZCS class E amplifier as electronic ballast are analysed in this paper. The presented study includes the selection of the best suited resonant tank and a parametric analysis of the ZCS class E amplifier.

Keywords: Electronic Ballast, ZCS, Class E Amplifier, Mathematica.

Resumen

En este artículo se propone el uso del amplificador clase E conmutado a corriente cero (CCC) como balastro electrónico para lámparas fluorescentes. El amplificador clase E CCC presenta un esfuerzo de voltaje en el interruptor más bajo que el amplificador clase E conmutado a voltaje cero (CVC). Esta es una ventaja importante que permite alimentar al circuito desde el voltaje de línea americano ($V_{ac}=120\text{ V}$), manteniendo sólo un interruptor en el balastro. En este artículo se analizan la operación y características del amplificador clase E CCC operando como balastro electrónico. El estudio incluye la selección del tanque resonante más apropiado y un análisis paramétrico del amplificador clase E CCC.

Palabras clave: Balastros Electrónicos, CCC, Amplificador Clase E, Matemática.

1 Introduction

The use of class E amplifiers to implement fluorescent lamp ballasts presents several interesting advantages as high power density, high efficiency and low component counts. However, the main disadvantage of these converters is the high voltage stress across the switch, which can reach a value as high as four times the input supply voltage. Until now, this disadvantage has limited the input voltage range of the class E amplifiers below 100 V, in order to avoid a high voltage stress across the switch obtained when supplying from a high main voltage. For instance, if a class E amplifier is supplied from American main voltage (120 Vrms), the voltage stress across the switch would be $V_{smax}=4*120*1.4142=648\text{ V}$, which means that a switch with a voltage rate of 1200 V must be used.

In order to solve this problem, in (Lütteke and Raets, 1986) and (Lütteke and Raets, 1987) the use of two switches in series, a bipolar and a MOSFET, operating as one only switch has been proposed. In this way, the resultant switch could bear a voltage stress up to 2 kV. However, with this solution the main problem of the converter is not resolved, since a considerable high voltage stress across the switch is maintained. Moreover, an extra floating switch is needed, which is not ground referenced, making necessary the use of an isolated driver.

An alternative solution to this problem of high voltage stress across the switch is to operate the switch with zero current switching instead of zero voltage switching provided by a conventional class E amplifier. With this goal, the use of a class E amplifier with a shunt inductor

has been proposed by Kazimierczuk (1981), which is the dual circuit of the conventional ZVS class E amplifier.

Thus, the switch voltage and current stresses under optimum operation for the ZCS class E amplifier are $V_{smax} = 2.862V_{cc}$ and $I_{smax} = 3.562I_{cc}$, whereas for the ZVS class E amplifier were $V_{smax} = 3.562V_{cc}$ and $I_{smax} = 2.862I_{cc}$. A voltage stress decrease of 19.65 % is then obtained thanks to the zero current switching feature. Therefore, this topology is an interesting option when the feeding voltage is the american main voltage ($V_{cc} = 180$ V) because allows the use of switches with a rated voltage of 600 V.

In this paper the operation of the ZCS class E inverter as fluorescent lamp ballast is analysed. The presented study is focused on the effect of parameter variations in the circuit operation and on the selection of the resonant tank best suited for handling fluorescent lamps.

2 Parametric Analysis

The analysis presented by Kazimierczuk (1981) considers only the optimum operation of the ZCS class E amplifier, this is, the operation with both zero current and zero slope switching. This is a very particular analysis, since there exists only one operation point satisfying this optimum switching. Thus, the class E amplifier could easily lose zero current switching operation if one or more circuit parameters are changed. The use of a diode in series or in parallel with the switch maintains the ZCS operation within a circuit parameter range, but the zero slope switching is lost (Kazimierczuk, 1989). A unidirectional switch will be employed in the proposed topology, implemented by using a diode in series with the switch. In this way, the parasitic capacitance will be lower than that existing in a bidirectional switch (which uses a diode in parallel), thus obtaining a reduction in the switch losses.

In this paper the circuit shown in Fig. 1, with a unidirectional current switch formed by a controlled switch with a series diode, is analysed under any operation conditions. A parametric analysis is performed to determine the variation range of the different circuit parameters maintaining zero current switching operation.

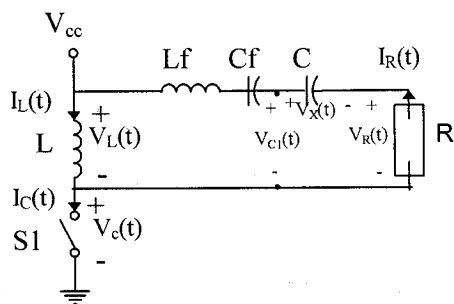


Fig. 1. ZCS Class E amplifier equivalent circuit

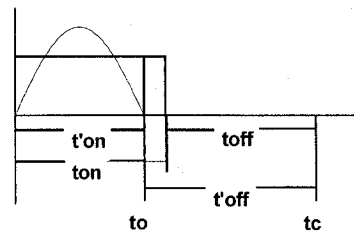


Fig. 2. Current waveform and signal control in the switch

Figure 1 shows the equivalent circuit of the ZCS class E amplifier used in this analysis. In this circuit the resonant capacitor C_r has been split into two different capacitors: C_f which is tuned with L_f and C . The resonant tank L_f-C_f is tuned at the switching frequency F . The quality factor $[Q = 1/(\omega R C_f)]$ is designed high enough to allow the output current to be assumed sinusoidal. In this analysis an ideal unidirectional switch S_1 is considered, which can only handle current in one direction. In this way, when the switch is reverse biased it behaves as an open switch without regarding the control signal. For this reason, two different duty cycles are obtained. Firstly, the duty cycle obtained from the control signal applied to the switch, which is considered equal to 50 % in this analysis, and secondly, the duty cycle given by the zero crossing of the current switch (D'). Figure 2 illustrates the two different duty cycles. In this figure the interval times t'_{on} and t'_{off} corresponds to the unidirectional switch duty cycle and the interval times t_{on} and t_{off} correspond to the control signal duty cycle. The unidirectional switch will start conducting at instant ωt_c , referred to the instant time t_0 , this angle can be expressed as follows:

$$\omega t_c = 2\pi(1 - D') \quad (1)$$

Furthermore, the switch is assumed ideal, this means that parasitic capacitances are neglected, the switch behaves as a short circuit and open circuit during the on and off states respectively, and the turn-on and turn-off transitions are instantaneous.

2.1 Voltage and Current in L and in S1

By inspecting Fig. 1 the voltage and current in the switch are given by the following expressions:

$$i_c(\omega t) = i_L(\omega t) - i_R(\omega t) \quad (2)$$

$$v_c(\omega t) = V_{cc} - v_L(\omega t) \quad (3)$$

When the switch is in the off state, it behaves as an open circuit. Therefore:

$$i_c(\omega t) = 0, \quad 0 \leq \omega t \leq \omega t_c \quad (4)$$

$$i_L(\omega t) = i_R(\omega t) = I_R \sin(\omega t + \phi) \quad 0 \leq \omega t \leq \omega t_c \quad (5)$$

$$v_L(\omega t) = \omega L \frac{di_L(\omega t)}{d(\omega t)} = \omega L I_R \cos(\omega t + \phi) \quad 0 \leq \omega t \leq \omega t_c \quad (6)$$

$$v_c(\omega t) = V_{cc} - \omega L I_R \cos(\omega t + \phi) \quad 0 \leq \omega t \leq \omega t_c \quad (7)$$

When the switch is in the on state, it behaves as a short circuit, then:

$$v_c(\omega t) = 0, \quad \omega t_c \leq \omega t \leq 2\pi \quad (8)$$

$$v_L(\omega t) = V_{cc} \quad \omega t_c \leq \omega t \leq 2\pi \quad (9)$$

Current through inductor L can be calculated as follows:

$$i_L(\omega t) = \frac{1}{\omega L} \int_{\omega t_c}^{\omega t} v_L(\omega t) d(\omega t) + i_L(\omega t_c +) \quad (10)$$

where $i_L(\omega t_c +)$ is the instantaneous inductor current during the turn-on transition of the switch, and its value is given by:

$$\begin{aligned} i_L(\omega t +) &= i_L(\omega t_c -) = I_R \text{sen}[2\pi(1-D') + \phi] \\ &= I_R \text{sen}(\phi - 2\pi D') \end{aligned} \quad (11)$$

By integrating (10) and using (11), the following expressions are obtained:

$$i_L(\omega t) = \frac{V_{cc}}{\omega L} [\omega t - 2\pi(1-D')] + I_R \text{sen}(\phi - 2\pi D') \quad \omega t_c \leq \omega t \leq 2\pi \quad (12)$$

$$i_c(\omega t) = \frac{V_{cc}}{\omega L} [\omega t - 2\pi(1-D')] + I_R \{ \text{sen}(\phi - 2\pi D') - \text{sen}(\omega t + \phi) \} \quad \omega t_c \leq \omega t \leq 2\pi \quad (13)$$

2.1.1 Resonant Tank Voltages

Since the resonant tank Lf-Cf is tuned at the switching frequency, it behaves as an ideal filter, allowing to circulate only the current given by the fundamental component of the voltage $v_L(t)$. Therefore, the voltage shown as $v_{c1}(t)$ in fig. 1 will be equal to the fundamental component of $v_L(t)$. This fundamental component is a sinusoidal waveform given by the following equation:

$$v_{c1}(\omega t) = \rho V_R \text{sen}(\omega t + \phi_1) \quad (14)$$

where V_R is the voltage amplitude across the load and:

$$\rho = \sqrt{1 + \frac{XC^2}{R^2}} \quad (15)$$

$$\phi_1 = \phi + \psi = \phi + \tan^{-1}\left(\frac{XC}{R}\right) \quad (16)$$

Regarding the voltage $v_{c1}(t)$ shown in Fig. 1, its fundamental component is calculated as follows:

$$\begin{aligned} V_{c1} &= \frac{2\pi(1-D')}{\pi} \int_0^{2\pi} [V_{cc} - \omega L I_R \cos(\omega t + \phi)] \text{sen}(\omega t + \phi_1) d(\omega t) \\ V_{c1} &= \frac{\omega L V_R}{4\pi R} [\cos(2D - \phi - \phi_1) - \cos(\phi + \phi_1) + (2D - 4\pi) \text{sen} \psi] - \\ &\quad - \frac{V_{cc}}{\pi} [\cos(D - \phi_1) - \cos \phi_1] \end{aligned} \quad (17)$$

where $D=2\pi D'$. By equalling (17) to the amplitude given by (14) and solving for V_R :

$$V_R = \frac{4V_{cc}R}{\omega L} \frac{[\cos(D - \phi_1) - \cos \phi_1]}{[\cos(2D - \phi - \phi_1) - \cos(\phi + \phi_1) + (2D - 4\pi) \text{sen} \psi - \frac{4\pi R \rho}{\omega L}]} \quad (18)$$

Equation (18) can also be expressed as follows:

$$V_R = \frac{4V_{cc}R}{\omega L} h(D, \phi, \phi_1, \psi, R, \rho, L) \quad (19)$$

where:

$$h(D, \phi, \psi, R, \rho, L) = \frac{\cos(D - \phi_1) - \cos \phi_1}{\cos(2D - \phi - \phi_1) - \cos(\phi + \phi_1) + (2D - 4\pi) \text{sen} \psi - \frac{4\pi R \rho}{\omega L}} \quad (20)$$

Since the fundamental component of voltage $v_{c1}(\omega t)$ has only a sinusoidal term, the cosinusoidal component must be equal to zero, this is:

$$\begin{aligned} 0 &= \frac{1}{\pi} \int_0^{2\pi(1-D')} V_c(\omega t) \cos(\omega t + \phi_1) d(\omega t) \\ 0 &= \frac{1}{\pi} \int_0^{2\pi(1-D')} \left[V_{cc} - \frac{\omega L V_R}{R} \cos(\omega t + \phi) \right] \cos(\omega t + \phi_1) d(\omega t) \end{aligned} \quad (21)$$

By integrating (21) and solving for V_R , the following expression is finally obtained:

$$V_R = \frac{4R V_{cc}}{\omega L} \frac{[\text{sen} \phi_1 + \text{sen}(D - \phi_1)]}{[(2D - 4\pi) \cos \psi + \text{sen}(2D - \phi - \phi_1) + \text{sen}(\phi + \phi_1)]} \quad (22)$$

Equation (22) can also be expressed in the following way:

$$V_R = \frac{4R V_{cc}}{\omega L} g(D, \phi, \phi_1, \psi, R) \quad (23)$$

where:

$$g(D, \phi) = \frac{\text{sen}(\phi_1) + \text{sen}(D - \phi_1)}{(2D - 4\pi) \cos \psi + \text{sen}(2D - \phi - \phi_1) + \text{sen}(\phi + \phi_1)} \quad (24)$$

By equalling (20) and (24), substituting $\phi_1 = \phi + \psi$ and expanding, the numerators and denominators of the functions $g()$ and $h()$ can be expressed as follows:

$$\begin{aligned}
g_{num} &= \text{sen}\phi(\cos\psi - \text{sen}D\text{sen}\psi - \cos D\cos\psi) + \\
&\quad \cos\phi(\text{sen}\psi + \text{sen}D\cos\psi - \cos D\text{sen}\psi) \\
h_{num} &= \text{sen}\phi(\text{sen}\psi - \cos D\text{sen}\psi + \text{sen}D\cos\psi) + \\
&\quad \cos\phi(\cos D\cos\psi - \cos\psi + \text{sen}D\text{sen}\psi) \\
g_{den} &= \text{sen}^2\phi(\text{sen}\psi\cos 2D - \text{sen}2D\cos\psi - \text{sen}\psi + (2D - 4\pi)\cos\psi) + \\
&\quad \text{sen}\phi\cos\phi(\cos\psi + \cos\psi - 2\text{sen}2D\text{sen}\psi - 2\cos 2D\cos\psi) + \\
&\quad \cos^2\phi[\text{sen}2D\cos\psi - \cos 2D\text{sen}\psi + \text{sen}\psi + (2d - 4\pi)\cos\psi] \\
h_{den} &= \text{sen}^2\phi\left(\cos\psi - \cos 2D\cos\psi - \text{sen}2D\text{sen}\psi + 2D\text{sen}\psi - 4\pi\text{sen}\psi - \frac{4\pi R\rho}{\omega L}\right) + \\
&\quad \cos^2\left(-\cos\psi + \text{sen}2D\text{sen}\psi + \cos 2D\cos\psi + 2D\text{sen}\psi - 4\pi\text{sen}\psi - \frac{4\pi R\rho}{\omega L}\right) + \\
&\quad \text{sen}\phi\cos\phi(2\text{sen}2D\cos\psi - 2\cos 2D\text{sen}\psi + 2\text{sen}\psi)
\end{aligned} \tag{25}$$

By assigning a new notation to each term multiplying to $\text{Sen}^2\phi$, $\text{Cos}^2\phi$, $\text{Sen}\phi\text{Cos}\phi$, as follows:

$$\begin{aligned}
q_1 &= \cos\psi - \text{sen}D\text{sen}\psi - \cos D\cos\psi \\
q_0 &= \text{sen}\psi + \text{sen}DCos\psi - \cos D\text{sen}\psi \\
r_2 &= \text{sen}\psi\cos 2D - \text{sen}2D\cos\psi - \text{sen}\psi + (2D - 4\pi)\cos\psi \\
r_1 &= \cos\psi + \cos\psi - 2\text{sen}2D\text{sen}\psi - 2\cos 2D\cos\psi \\
r_0 &= \text{sen}2D\cos\psi - \cos 2D\text{sen}\psi + \text{sen}\psi + (2d - 4\pi)\cos\psi \\
s_2 &= \cos\psi - \cos 2D\cos\psi - \text{sen}2D\text{sen}\psi + 2D\text{sen}\psi - 4\pi\text{sen}\psi - \frac{4\pi R\rho}{\omega L} \\
s_1 &= 2\text{sen}2D\cos\psi - 2\cos 2D\text{sen}\psi + 2\text{sen}\psi \\
s_0 &= -\cos\psi + \text{sen}2D\text{sen}\psi + \cos 2D\cos\psi + 2D\text{sen}\psi - 4\pi\text{sen}\psi - \frac{4\pi R\rho}{\omega L}
\end{aligned} \tag{26}$$

Then, equations corresponding to the functions $g()$ and $h()$ can be expressed in the following way:

$$\begin{aligned}
g_{num} &= q_1 \text{sen}\phi + q_0 \cos\phi \\
g_{den} &= r_2 \text{sen}^2\phi + r_1 \text{sen}\phi\cos\phi + r_0 \cos^2\phi \\
h_{num} &= q_0 \text{sen}\phi - q_1 \cos\phi \\
h_{den} &= S_2 \text{sen}^2\phi + S_1 \text{sen}\phi\cos\phi + S_0 \cos^2\phi
\end{aligned} \tag{27}$$

Taking into account the following condition:

$$\frac{g_{num}}{g_{den}} = \frac{h_{num}}{h_{den}}$$

which is the same as:

$$g_{num}h_{den} - g_{den}h_{num} = 0$$

by substituting (27), multiplying and expanding:

$$\alpha_3 \text{sen}^3\phi + \alpha_2 \text{sen}^2\phi\cos\phi + \alpha_1 \text{sen}\phi\cos^2\phi + \alpha_0 \cos^3\phi = 0 \tag{28}$$

where:

$$\begin{aligned}
\alpha_3 &= q_1s_2 - r_2q_0 \\
\alpha_2 &= q_1s_1 + q_0s_2 + r_2q_1 - r_1q_0 \\
\alpha_1 &= q_1s_0 + q_0s_1 + r_1q_1 - r_0q_0 \\
\alpha_0 &= q_0s_0 + r_0q_1
\end{aligned} \tag{29}$$

Multiplying both sides of (28) by $\cos^3\phi$, we obtain:

$$\alpha_3 \tan^3\phi + \alpha_2 \tan^2\phi + \alpha_1 \tan\phi + \alpha_0 = 0 \tag{30}$$

Dividing (30) by α_3 :

$$\tan^3\phi + \frac{\alpha_2}{\alpha_3} \tan^2\phi + \frac{\alpha_1}{\alpha_3} \tan\phi + \frac{\alpha_0}{\alpha_3} = 0 \tag{31}$$

Since $\alpha_1 = \alpha_3$ and $\alpha_0 = \alpha_2$:

$$\tan^3\phi + \frac{\alpha_2}{\alpha_3} \tan^2\phi + \tan\phi + \frac{\alpha_2}{\alpha_3} = 0 \tag{32}$$

Factorising (32), we obtain:

$$\left(\tan\phi + \frac{\alpha_2}{\alpha_3}\right)(\tan^2\phi + 1) = 0$$

The first factor contains the real root of ϕ , therefore:

$$\phi = \arctan\left(-\frac{\alpha_2}{\alpha_3}\right) = \arctan\left(-\frac{\alpha_0}{\alpha_1}\right) \tag{33}$$

Once the ϕ angle has been obtained, it is possible to calculate any parameter of the class E amplifier under any operation condition.

2.2 Calculation of the D' duty Cycle

The current through the switch is given by (13). The zero crossing of the switch-diode current occurs for an angle equal to 2π . Therefore:

$$0 = \frac{V_{cc}}{2XL\pi D'} + I_R(\text{sen}(\phi - 2\pi D') - \text{sen}(\phi)) \tag{34}$$

In this equation the only independent variable is the duty cycle D' . Consequently, with this equation and by using numerical methods the duty cycle D' can be calculated.

2.3 Voltage and Current Stresses in the Switch

The peak current can be obtained by equalling to zero the derivative of (13) and solving for the angle of interest. This angle will indicate the instant of maximum current and is given by the following equation:

$$\theta_{MI} = -\cos^{-1}\left(\frac{V_{cc}}{I_R XL}\right) - \phi + 2\pi \tag{35}$$

By using (35) in (13) the maximum value of the switch current is obtained.

Regarding the peak voltage across the switch, the same procedure is followed with equation (7), in this case the peak voltage angle is the following:

$$\theta_{MV} = \pi - \phi \tag{36}$$

2.4 Average Input Current

The average current delivered by the power supply to the ZCS class E amplifier is obtained by integrating (4) and (13) within a period. The result is given by the following equation:

$$I_{cc} = \frac{D^2 \pi V_{cc}}{XL} + \frac{I_R}{2\pi(\cos\phi - \cos(\phi - 2\pi D') + 2D' \pi \sin(\phi - 2D' \pi))} \quad (37)$$

2.5 Input and Output Power and Power Capability

The input power is given by the following equation:

$$P_{in} = V_{cc} I_{cc} \quad (38)$$

and the output power can be calculated as follows:

$$P_o = \frac{I_R^2}{2} R \quad (39)$$

The power capability is a quantity which evaluate the ratio of the output power to the voltage and current stresses and is given by the following expression:

$$C_p = \frac{P_o}{I_{CM} V_{CM}} \quad (40)$$

being I_{CM} and V_{CM} he maximum current and voltage through the switch respectively.

Previous equations were introduced in a Mathematica program (see appendix A), in order to evaluate the circuit behaviour under suboptimum operation and using a diode in series with the transistor. Using this program the operation of the class E amplifier under variations on the following parameters: R, L, equivalent series capacitance of the resonant tank C and switching frequency F was performed (see fig. 1). Note that changes in Lf or Cf are reflected as changes in capacitor C, and thus considered as variations in C. In order to simplify the analysis, the different parameters were normalised using the optimum values previously calculated in by Kazimierczuk (1981): $R=1$, $F=1$, $V_{cc}=1$, $L=(\pi^2+4)/16$ y $C=16/(2\pi^2(\pi^2+12))$.

The algorithm performed by the Mathematica program shown in Appendix A can be summarised in the following steps:

1. Supply the values of the different circuit elements and per unit specifications
2. Calculate the phase angle between load voltage and control signal (ϕ), given by (33)
3. Calculate the duty cycle
4. Calculate maximum switch voltage and current
5. Calculate the average input current consumed by the ZCS class E amplifier
6. Display results and plot switch waveforms

As result of the performed analysis the following variations in the different elements of the class E

amplifier were found to maintain ZCS operation: $0 < R \leq 1$, $1 \leq F \leq 1.15$, $1 \leq L \leq 1.45$ and $1 \leq C \leq 1.28$. Figures 3 to 7 illustrate the results obtained from the performed analysis for variations in the load resistance R. Figure 3 shows the switch current waveform, Fig. 4 illustrates the switch voltage waveform, Fig. 5 shows the maximum voltage and current stresses and finally, Fig. 6 represents the load voltage amplitude. Similar waveforms can be obtained for changes in L, F and C.

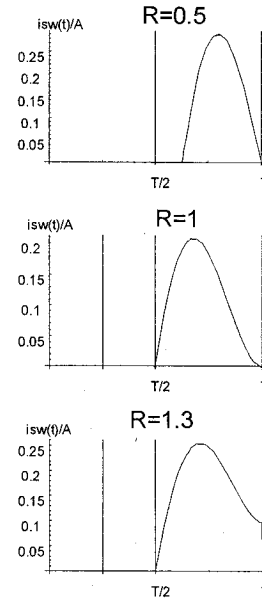


Fig. 3. Current waveform across the switch for variations of R

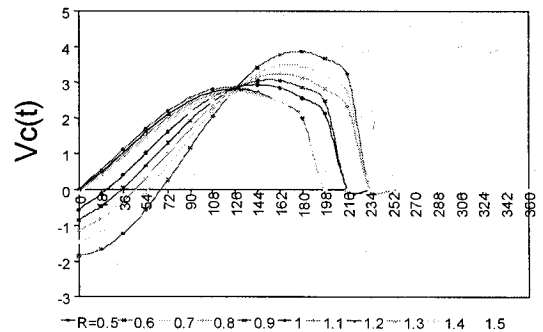


Fig. 4. Voltage waveform for variations of R

As conclusion of the performed analysis, the ZCS class E amplifier can accept quite well a parameter variation, particularly in the load resistance R, without loosing ZCS operation, provided that a diode is used in series with the transistor. These results are similar to those obtained by Raab (1978) for the ZVS class E amplifier. In all cases in which ZCS operation was maintained, the switch voltage stress was higher to that obtained for optimum operation (zero current and zero slope switching). The switch voltage stress only decreased when ZCS operation was lost.

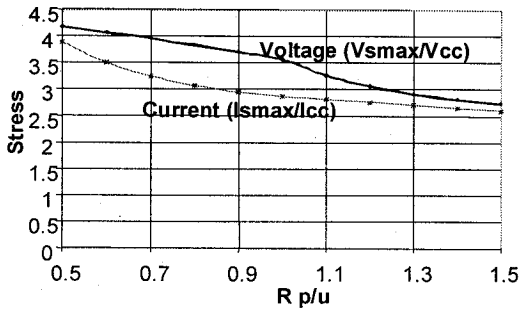


Fig. 5. Maximum stress voltage and maximum stress current vs R

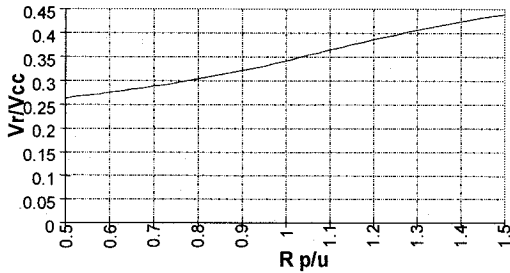


Fig. 6. Load voltage (V_r p/u) vs. R

2.6 Analysis of Losses in the Switch

In the previous analysis the switch was considered ideal, and only the turn-off losses due to non-zero current switching were evaluated. These losses are given by the energy stored in L at the instant of the commutation and generated during the switch turn-off process. However, for a real switch, the following energy losses should be also taking into account:

Conduction losses. Generated by the equivalent resistance of a saturated MOSFET (R_{on}) or by the equivalent voltage source of a saturated power BJT or IGBT (V_{ces}).

Transistor turn-on losses. In this particular topology these losses are given by the parasitic capacitance in parallel with the switch and it is composed by the switch output capacitance (C_{oss}), inductor L parasitic capacitance and the capacitance of the drain (or collector) connections to ground and power supply. The different losses will be now evaluated.

2.7 MOSFET Conduction Losses

($P_{R(on)}$)

The conduction losses due to the equivalent on resistance of a MOSFET can be easily obtained from the following equation:

$$P_{R(on)} = \frac{1}{2\pi} \int_{-\pi}^{\pi} i_c(\omega t)^2 R_{ON} dt \quad (41)$$

where R_{ON} is the equivalent on resistance and $i_c(\omega t)$ is the drain current for a duty cycle of 50%.

The drain current is given by the following expression (Kazimierzuk, 1981):

$$i_c(\omega t) = \frac{V_{cc}}{\omega L} \left(\omega t - \frac{3\pi}{2} - \frac{\pi}{2} \cos \omega t - \sin \omega t \right) \quad (42)$$

Using $i_c(\omega t)$ in (41) and solving:

$$P_{R(on)} = R_{ON} \left[\frac{V_{CC}^2}{2(\omega L)^2} \left(9 + 17\pi^2 - 27 - \frac{29\pi^2}{2} \right) \right] \quad (43)$$

Simplifying, we obtain:

$$P_{R(on)} = \frac{R_{ON} V_{CC}^2}{2(\omega L)^2} \left(\frac{5\pi^2}{2} - 18 \right) \quad (44)$$

The term $(\omega L)^2$ can be expressed as a function of the series load resistance according to the following expression (Kazimierzuk, 1981):

$$(\omega L)^2 = 29.665451 R^2 \quad (45)$$

Thus, equation (44) can be written as follows:

$$P_{R(on)} = \frac{R_{ON} V_{CC}^2 (0.112487)}{R^2} \quad (46)$$

Also, the series resistance R can be expressed as a function of the output power (Kazimierzuk, 1981), as follows:

$$R = 0.05844 \frac{V_{CC}^2}{P_{sal}} \quad (47)$$

Using (47) in (46) the following expression is finally derived for the conduction losses:

$$P_{R(on)} = \frac{32.9368 R_{ON} P_s^2}{V_{CC}^2} \quad (48)$$

Equation (48) yields the conduction losses for a given MOSFET and a given power and input voltages. For instance, for a IRF840 MOSFET with $R_{on}=0.85 \Omega$, a power $P_s=32$ W and an input voltage $V_{cc}=180$ V the calculated conduction losses are 0.88W.

2.8 BJT or IGBT Conduction Losses

The conduction losses of a BJT or a IGBT can be obtained from the equivalent on voltage V_{ce} by using the following expression:

$$P_{VCE} = \frac{1}{2\pi} \int_{-\pi}^{\pi} I_c(\omega t) V_{CE} d\omega t \quad (49)$$

where $i_C(\omega t)$ is the collector current for a 50% duty cycle. The collector current is given by the following equation:

$$i_C(\omega t) = \frac{V_{CC}}{\omega L} \left(\omega t - \frac{3\pi}{2} - \frac{\pi}{2} \cos \omega t - \sin \omega t \right) \quad (50)$$

Using $i_C(\omega t)$ in (49) and solving we obtain:

$$P_{VCE} = \frac{V_{CC} V_{CE}}{\pi \omega L} \quad (51)$$

Thus, equation (51) can be written as follows:

$$P_{VCE} = \frac{V_{CC} V_{CE}}{17.111R} \quad (52)$$

Using (47) in (52) the following expression is finally obtained:

$$P_{VCE} = \frac{V_{CE} P_{sal}}{V_{CC}} \quad (53)$$

For a IRGPH50F, the maximum on equivalent voltage is 2.9 V, for $V_{CC}=180$ V and $P_s=32$ W, a power of $P_{VCE}=0.515$ W is calculated.

As can be seen, the conduction losses are lower for an IGBT than for a MOSFET. This is a reasonable conclusion, since the MOSFET losses depends on the square of the supply voltage, whereas the IGBT losses depends linearly on the supply voltage. Considering only the conduction losses, it is more adequate the use of IGBTs than the use of a MOSFET for the proposed topology. The main drawback of the IGBTs is the lower switching frequency range in which they can be operated. However, this disadvantage is not very important in this topology since the high parasitic capacitance of the switch prevents from operating at high frequencies.

2.9 Switch Turn-on Losses

These losses are mainly given by the energy stored in the parasitic capacitance existing across the switch. These losses can be expressed as follows:

$$P_{CP} = \frac{1}{2} V_C^2 C_p f \quad (54)$$

where V_C is the voltage across the parasitic capacitor at the turn-on instant, C_p is the equivalent parasitic capacitance of the switch during the off state and f is the switching frequency. For an optimum commutation with a 50% duty cycle, the charging voltage of C_p is twice the supply voltage $V_C=2 V_{CC}$. Thus, equation (54) can be expressed as:

$$P_{CP} = 2V_{CC}^2 C_p f \quad (55)$$

For an IGBT IRGPH50F the parasitic capacitance C_p is $C_p=C_{oss}=340$ pF, a switching frequency $f=100$ kHz and $V_{CC}=180$ V the power is $P_{CP}=2.2$ W.

As can be seen, losses given by C_p highly contribute to the total circuit losses, and it is important to find solutions to reduce these losses. The parasitic capacitance depends on the type of switch used, what means that a switch with the lower C_p should be selected. Another way to reduce these losses is by operating at a lower switching frequency.

3 Selection of the Resonant Tank

The capability to accommodate high load variations is one of the important conditions in order to use an inverter as fluorescent lamp ballast. Thus, the inverter must tolerate load variations from a very high impedance load when the lamp is not ignited, to the nominal load impedance when the lamp is running. According to the performed parametric analysis for the ZCS class E amplifier, this topology can undergo load variations from the nominal load down to zero without loosing zero current switching, which is the opposite behaviour as necessary for a lamp ballast. In order to solve this problem an impedance inverter is used, thus reflecting a high load impedance as a low load impedance towards the ZCS class E amplifier. There exist two possibilities in order to implement the impedance inverter: the capacitive impedance inverter (Fig. 7a) and the LCC resonant tank (Fig. 7b). Both circuits are useful to perform the impedance inversion. However, to calculate the resonant tank elements two conditions must also be satisfied: a) to achieve lamp ignition and b) to supply the lamp at nominal power. For the LCC resonant tank, when trying to satisfy both conditions at constant switching frequency, the following constrain is obtained (Ponce, 1999):

$$V_1 \geq \sqrt{2P_L R_{se}} \quad (56)$$

Where V_1 is the fundamental component of the voltage applied to the resonant tank, P_L is the lamp power and R_{se} is the equivalent series resistance of the resonant tank and load.

For the following operation conditions: $P_L=32$ W, $R_L=132 \Omega$, main voltage of $120V_{rms}$ and minimum lamp ignition voltage of 350 V, the constrain given by (56) can not be satisfied. Therefore, the LCC resonant tank can not be employed.

The capacitive impedance inverter avoid this constrain. Besides, it presents a higher voltage boost ratio than the LCC resonant tank, since one capacitor is in series with the load instead of the input power supply, as in the LCC resonant tank. Therefore, the capacitive impedance inverter is chosen as the more appropriate resonant tank for this topology.

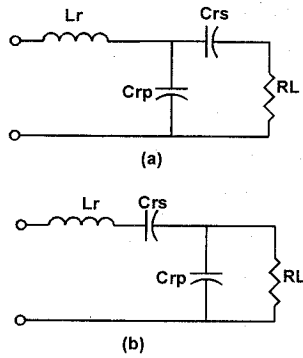


Fig. 7. Impedance inverters. (a) capacitive impedance inverter, (b) LCC resonant tank

4 Simplified Design of a ZCS Class E Amplifier

The procedure to calculate the different components of the class E amplifier consists of two steps. Firstly, the calculation of the ZCS class E amplifier elements, when loaded with a series resonant tank. Secondly, the calculation of the capacitive impedance inverter elements.

The input specifications to calculate the different elements are the following: $V_{ca}=127$ Vrms, $P_L=32$ W, $R_L=132$, $F=100$ kHz and quality factor $Q=10$.

Using the equations given by Kazimierczuk (1981) the following results were obtained: $R_e=63.11$ Ω , $L=547$ μ H, $C_r=2.521$ nF y $L_r=573.11$ μ H.

In order to calculate the elements of the capacitive impedance inverter, the circuit was simplified assuming an equivalent series circuit. Based on the circuit analysis, the relationship between the capacitive impedance inverter and a series resonant tank are obtained as follows:

$$R_e = \frac{R_L X C_{rp}^2}{R_L^2 + (X C_{rp} + X C_{rs})^2} \quad (57)$$

$$X C_{se} = \frac{X C_{rp} (R_L^2 + X C_{rp} X C_{rs} + X C_{rs}^2)}{R_L^2 + (X C_{rp} + X C_{rs})^2} \quad (58)$$

Where R_e and $X C_{se}$ are the equivalent series resistance and series capacitance and are known values, R_L is the equivalent lamp resistance and $X C_{rp}$ and $X C_{rs}$ are the reactances of C_{rp} and C_{rs} respectively.

Solving (57) and (58) for $X C_{rs}$ and $X C_{rp}$, the values of the capacitors can be obtained. In this example the following values are obtained: $C_{rs}=766$ pF and $C_{rp}=1.77$ nF.

The diagram of the implemented prototype is shown in figure 8. The switch employed was an IGBT IRG4BC30UD with a rated voltage of 600 V.

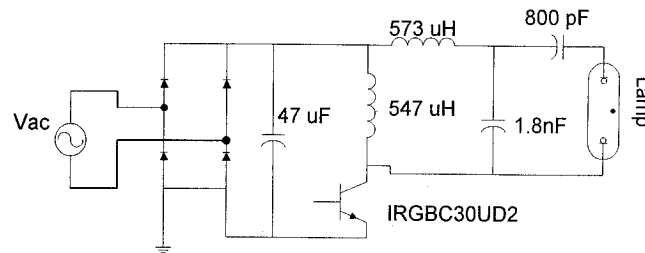


Fig. 8. Electronic ballast based on the ZCS class E amplifier

5 Experimental Results

The designed prototype was implemented and tested with the following results: Figure 9 shows the current and voltage stresses in the switch obtained with the proposed electronic ballast. As can be seen in this figure, the maximum voltage stress across the switch is 540 V (lower that the rated voltage of the switch), the oscillations in the switch voltage waveform are due to the resonance between the parasitic capacitance and the inductor L . The current waveform is sinusoidal with zero current switching (ZCS) at the turn on and turn off of the switch, the maximum current troughs the switch is 1.22 A.

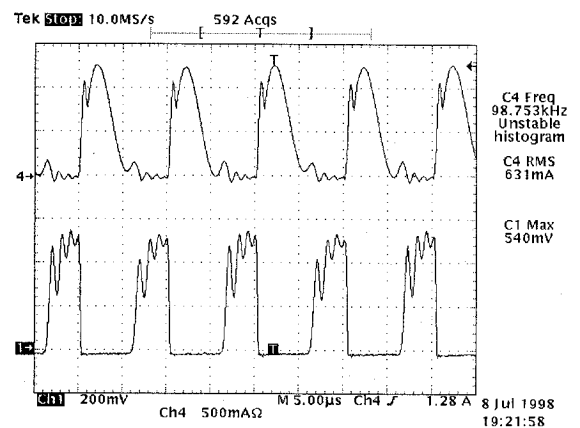


Fig. 9. Switch current waveform (upper trace: 500 mA/div, 5 us/div) and switch voltage waveform (lower trace, 200 V/div, 5 us/div)

Figure 10 illustrates the lamp current waveform; as can be seen in this figure, the current is symmetrical and almost sinusoidal. The lamp current waveform can be improved increasing the quality factor, but the efficiency will be lower. The measured lamp current crest factor was 1.8 and the measured efficiency was 70 %.

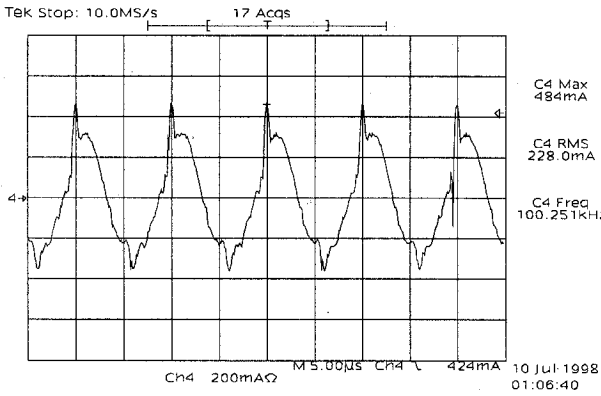


Figure 10. Lamp current waveform 200 mA/div, 5 us/div

The lower efficiency obtained is mainly due to the fact that the ZCS class E amplifier presents high losses generated by the parasitic capacitor across the switch. Furthermore, for the correct operation of this topology, a high quality factor is necessary, in this case we use $Q=10$, by this reason the losses in the inductors are more significant. Table I provides an estimation of the main energy losses in the different components of the ZCS class E amplifier, expressed as a percentage of the total input power.

Component	% losses
L	6
Lr	6
Turn-on (Cp losses)	12
Turn-off	4
On losses	2

Table I. Estimated loss distribution in the ZCS class E amplifier

6 Conclusions

In this paper the ZCS class E amplifier is proposed as fluorescent lamp electronic ballast featuring low voltage stress when compared to the ZVS class E amplifier. With this goal a parametric analysis of the ZCS class E amplifier was performed and the use of a capacitive impedance inverter as resonant tank was suggested. For the parametric analysis of the ZCS class E amplifier a diode in series with the switch was considered. With this analysis the variation range of the different circuit elements assuring zero current switching was determined and the relevant equations to evaluate the operation of the ZCS class E amplifier under any operation condition were derived.

Based on the presented study, an electronic ballast for a 32W compact fluorescent lamp was designed and experimental results were obtained to verify the described behaviour. With the proposed circuit an electronic ballast able to be supplied from the american main voltage ($V_{cc}=180$ V) and using only one switch with a voltage stress below 600 V can be implemented.

Appendix A

MATHEMATICA PROGRAM FOR THE PARAMETRIC ANALYSIS OF THE PROPOSED TOPOLOGY

```
(* Input variables, Ce is C *)
Vcc=1; (*Source voltage p/u*)
R=1; (*Load series resistance p/u*)
f=1; (*Switching frequency p/u*)
w=2 Pi f; (*Angular frequency*)
L=N[(Pi^2+4)/16]; (*Shunt inductor p/u, optimum value*)
XL=L w; (*Reactance of L*)
Ce=N[16/(2 Pi^2 (Pi^2+12))]; (*Excessive capacitance of the resonant tank C*)
Xc=-1/w/Ce; (*Reactance of C or Ce*)
(* Calculation of Phi *)
ro=N[ Sqrt[1+Xc^2/R^2]];
Psi=N[ArcTan[Xc/R]];
r2:=N[ Sin[Psi] Cos[2 D1]-Sin[2 D1] Cos[Psi]-Sin[Psi]+(2 D1-4 Pi) Cos[Psi]];
r1:=N[2 Cos[Psi]-2 Sin[2 D1] Sin[Psi]-2 Cos[2 D1] Cos[Psi]];
r0:=N[ Sin[2 D1] Cos[Psi]-Cos[2 D1] Sin[Psi]+Sin[Psi]+(2 D1-4 Pi) Cos[Psi]];
s2:=N[ Cos[Psi]-Cos[2 D1] Cos[Psi]-Sin[2 D1] Sin[Psi]+2 D1 Sin[Psi]-4 Pi Sin[Psi]-4 Pi R ro/XL];
s1:=N[2 Sin[2 D1] Cos[Psi]-2 Cos[2 D1] Sin[Psi]+2 Sin[Psi]];
s0:=N[-Cos[Psi]+Sin[2 D1] Sin[Psi]+Cos[2 D1] Cos[Psi]+2 D1 Sin[Psi]-4 Pi Sin[Psi]-4 Pi R ro/XL];
q1:=N[ Cos[Psi]-Sin[D1] Sin[Psi]-Cos[D1] Cos[Psi]];
q0:=N[ Sin[Psi]+Sin[D1] Cos[Psi]-Cos[D1] Sin[Psi]];
al3:=q1 s2-r2 q0;
al2:=q1 s1+q0 s2+r2 q1-r1 q0;
al1:=q1 s0+q0 s1+r1 q1-r0 q0;
al0:=q0 s0+r0 q1;
phi:=N[ArcTan[-al2/al3]];
phi1=N[phi+Psi];
Vr:=N[4 Vcc R (Cos[D1-phi1]-Cos[phi1])/XL/(Cos[2 D1-phi-phi1]-Cos[phi+phi1]+(2 D1-4 Pi)Sin[Psi]-4 Pi R ro/XL)]; (*Voltage on R*)
D2:=D1/2 /Pi; (*Effective duty cycle D2=D*)
phi:=N[ArcTan[-al2/al3]];
(* Calculation of the Duty cycle *)
Ic:=Vcc/(2 XL Pi D2)+Vr/R/(Sin[phi-2 Pi D2]-Sin[phi]);
Plot[Ic,{D1,Pi/2,1.5 Pi}]; (*Getting the initial condition of the Duty cycle*)
Ic:=Vcc/XL(2 Pi D2)+Vr/R/(Sin[phi-2 Pi D2]-Sin[phi]);
res=FindRoot[Ic==0,{D1,2}];
D1=D1/res;
Print["D2=",N[D2]]
(* Maximum current trough the switch *)
thm=(-ArcCos[Vcc R/Vr/XL]-phi+2 Pi);
Icmax=N[Vcc/XL(thm-2 Pi(1-D2))+Vr/R (Sin[phi-2 Pi D2]-Sin[thm+phi])];
(* Maximum voltage across the switch *)
thm1=Pi-phi;
Vcm=Vcc-XL Vr/R Cos[thm1+phi];
(* Average input current *)
Icc=D2^2 Pi Vcc/XL +Vr/R/2/Pi(Cos[phi]-Cos[phi-2 D2 Pi]+2 D2 Pi Sin[phi-2 D2 Pi]);
(* Input and output power *)
Pin=Vcc Icc;
Po=Vr^2/2/R;
Cp=Po/Icmax/Vcm;
(* Calculated values *)
Print["phi=",N[phi]];
Print["D'=",N[D2]];
Print["Vr=",Vr];
Print["Ismáx=",N[Icmax/Icc]];
Print["Vcmáx=",N[Vcm/Vcc]];
Print["Icc=",N[Icc]];
Print["Pin=",N[Pin]];
Print["Po=",N[Po]];
Print["Cp=",N[Cp]];
(*Plotting the waveforms of voltage and current in the switch *)
Vcoff[t_]:=If[0<=t<=(2 N[Pi]-N[D1]),Vcc-XL Vr/R Cos[t+phi],0];
ic[t_]:=If[(2 N[Pi]-N[D1])<t<2 Pi,Vcc/XL (t-2 Pi(1-D2))+Vr/R (Sin[phi-2 Pi D2]-Sin[t+phi]),0];
tperiod=2 Pi;
Plot[Vc[t],{t,0,2 N[Pi]},AxesLabel->{"time","isw(t)/A"},
Ticks->{{1/4 tperiod,""},{1/2 tperiod,"T/2"},{3/4 tperiod,""},{tperiod,"T"}},
Automatic], PlotLabel->"Current in the switch",GridLines->{{tperiod,1/4 tperiod,1/2 tperiod,tperiod},None}];
Plot[Vc[t],{t,0,2 N[Pi]},AxesLabel->{"time","isw(t)/A"},
Ticks->{{1/4 tperiod,""},{1/2 tperiod,"T/2"},{3/4 tperiod,""},{tperiod,"T"}},
Automatic], PlotLabel->"Voltage trough the switch",GridLines->{{tperiod,1/4 tperiod,1/2 tperiod,tperiod},None}];
```

References

Kazimierczuk M., "Class E Tuned Power Amplifier with Shunt Inductor", IEEE Journal of Solid-State Circuits, Vol. SC-16, No. 1, Feb 1981, pp. 2-7.

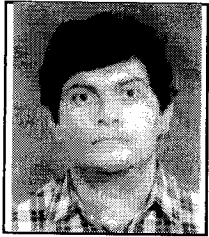
Kazimierczuk M. K., and **K. Puczek**. "Class E Tuned Power Amplifier with Antiparallel Diode or Series Diode at Switch, with any Loaded Q and Switch Duty Cycle", IEEE Transactions on Circuits and Systems, Vol. 36, No. 9, (September 1989), pp. 1201-1209.

Lütteke G., and **H. C. Raets**. "High Voltage High Frequency Class-E Converter Suitable for Miniaturisation". IEEE Transactions on Power Electronics, Vol. PE-1, No. 4, Oct. 1986, pp. 193-199.

Lütteke G., and **H. C. Raets**. "220-V Mains 500 kHz Class-E Converter Using a BIMOS". IEEE Transactions on Power Electronics, Vol. PE-2, No. 3, Jul. 1987, pp. 186-193.

Ponce M., "Power Supply for Discharge Lamps Based on Class E Amplifiers", Ph. D. Thesis, CENIDET, 1999. In Spanish.

Raab F. H., "Effects of Circuit Variations on the Class E Tuned Power Amplifier". IEEE Journal of Solid-State Circuits, Vol. SC-13, No 2, (Abril 1978), pp. 239-247.



Mario Ponce, he received the Bachelor Engineer Electrical degree from the San Luis Potosí Autonomous University (1993), M.Sc. degree from CENIDET (1996) and Ph. D. degree from CENIDET (1999). Nowadays, he is Full time Associate - Professor and Researcher at CENIDET since March 1999. He has published more than 20 papers in magazines, journals and international conferences in power electronics.



Rubén Vázquez, he received the Bachelor Engineer Electrical degree from the Instituto Tecnológico de Minatitlan (1996) and M.Sc. degree from CENIDET (1998). Nowadays, he is Full time Associate - Professor at the Instituto Tecnológico de Minatitlan.



Jaime E. Arau, he obtained his BSc degree in Electronics Engineering from the Instituto Tecnológico de Minatitlan, Mexico (1982) and the PhD degree in Power Electronics from the Universidad Politécnica de Madrid, Spain (1991). He was Head of the Electronics Department at the National Center for Research and Technological Development (CENIDET). He is currently a full time professor and the CENIDET Academic Vice-Director. Dr. Arau has around 70 journals and international conferences papers and more than 60 in national ones. Inside the IEEE, Dr. Arau is Senior member (since 1997), President of the IEEE Section Morelos (1997-1998), as well as Member at Large (1998-2000), Region 9 Liaison (1996-1997), and Chapters Developments Chair (since January 1999) of the IEEE Power Electronics Society (PELS) AdCom. He is member of the Technical Committee of different worldwide recognized conferences as the IEEE Power Electronics Specialists Conference - PESC (since 1995) and the IEEE Applied Power Electronics Conference and Exhibition - APEC (since 1997). In February 2000, received the IEEE Third Millennium Medal.



J. Marcos Alonso, he received the MSc. Degree in electrical engineering in 1990 from the University of Oviedo, Spain. In 1994 he received the Ph. Degree from the same University. Assistant professor of the university of Oviedo between 1990-1999. Since 1999 he is an Associate Professor at the Electrical and Electronic Department of the University of Oviedo. He is the primary author for more than 30 journal and international conference papers in power and industrial electronics. His research interests include high-frequency electronic ballasts, discharge lamp modeling, power factor correction topologies, high frequency switching converters, power converters for electrostatic applications and industrial control systems. He currently holds two Spanish patents and has other four pending. Dr. Alonso is a recipient of the IEEE Industrial Electronics Society Meritorious Paper Award for 1996. He is an active member of the Institute of Electrical and Electronics Engineers (IEEE), where he collaborates as transactions paper reviewer, conference session chairman and other. He is also member of the International Ozone Association (IOA).

